



Studies on Chemical synthesis and Structural, Morphological and Optical Properties of ZnO Nanorods

¹Anju Singh, ²H.L.Vishwakarma

¹Department of Physics, R.C.E.T, Bhilai (C.G.), INDIA

²Department of Physics, Sarguja University, Ambikapur (C.G.), INDIA

Email: ¹Singh_nk24@yahoo.com, ²horilal5@yahoo.com

Abstract : Zinc Oxide (ZnO) nanorods have been achieved by a simple chemical precipitation method at room temperature. Poly Vinyl Pyrrolidone (PVP) is used as a capping agent. X-Ray Diffraction (XRD) result shows that the synthesized undoped ZnO nanorods have wurtzite hexagonal structure without any impurities. It has been seen that the growth orientation of the prepared ZnO nanorods were (101). XRD analysis revealed that the nanorods have the crystallite size 49 nm. Debye Scherrer formula is used for calculating the crystalline size and Williamson Hall equation is used for calculating the lattice strain. Cell volume, Lorentz factor, Lorentz polarization factor, bond length, texture coefficient, lattice constants and dislocation density are also studied. Here, we also

I. INTRODUCTION

In recent years one dimensional nanostructure materials like nanorods, nanowires and nanotubes have received more attention due to their remarkable properties. These properties are very useful in all fields like optoelectronics, electronic nanodevices etc. [1]-[2]. To understand the basic phenomena of quantum size effect on electrical, optical, mechanical and magnetic properties, some important semiconductor nanomaterials like GaN[3], CdS[4], Si[5], SnO₂[6], TiO₂[7], ZnO[8,9] and CeO₂[10-13] have been widely studied. Among them ZnO nanomaterials have been chosen because of their remarkable properties like wide and direct bandgap ($E_g \sim 3.4$ eV) and large exciton binding energy (60 meV). UV lasing action is possible at room temperature due to wide bandgap and large exciton binding energy as explained by [14]. In ZnO, due to the extreme large binding energy, the excitons are thermally stable. Due to all these reasons ZnO has significant advantages in optoelectronic applications like ultraviolet (UV) lasing media [15]. The wide and direct optical energy band gap of 3.37 eV is large enough to transmit most of the useful solar radiation for ZnO. ZnO is an n-type semiconductor belonging to II-VI group which is very useful for transparent electrodes in flat panel displays, solar cells and promising material for short wavelength light emitting devices [16]-[18]. Its epitaxial films and nanostructures have been mostly studied for its applications in UV-emitters, solar cells, gas sensors,

compared the interplaner spacing and relative peak intensities from their standard values with different angles. The Scanning Electron Microscope (SEM) image confirmed the size and shape of these nanorods. It has been found that the diameter of nanorods ranges from 1.52 μm to 1.61 μm and the length about 4.89 μm . At room temperature Ultraviolet Visible (UV-Vis) absorption band has been observed around 355 nm (blue shifted as compared to bulk). The average particle size is also calculated by mathematical model of effective mass approximation equation by using UV-Visible absorption peak. Finally, the bandgap is calculated by UV-absorption peak.

Keywords: Optoelectronic, bandgap, nanorods, zinc oxide varistors and surface electro-acoustic wave devices as given by [19]. Low dimensional nanostructures are now being extensively used in the field of advanced devices.

For the synthesis of nanomaterials there are various methods like chemical vapour deposition [20], laser ablation [21], vacuum arc deposition [22], sputtering [23] and hydrothermal process [24]-[25]. But most of these fabrication techniques have complex steps, which require extremely sophisticated instruments, precise experimental setup and extreme experimental conditions. Hence, it is important to develop a very simple method to fabricate ZnO nanorods in laboratory environment. The chemical precipitation method provides a better route to fabricate multidimensional nanostructure in a very large scale. This technique is inexpensive, which does not require any complicated processing or huge infrastructures.

In this study, chemical precipitation method is used for synthesis of zinc oxide nanorods at room temperature. Further the samples are characterized by XRD and SEM; optical properties are also discussed by UV-VIS spectroscopy.

II. EXPERIMENTAL

A. Materials

Zinc Acetate Dihydrate $\text{Zn}(\text{CH}_3\text{COO})_2 \cdot 2\text{H}_2\text{O}$, Sodium Hydroxide (NaOH), Poly Vinyl Pyrrolidone (PVP) and absolute ethanol were used to synthesize undoped zinc

oxide nanorods. All these chemicals were used as precursors which were obtained from MERCK chemical company. PVP was used as a capping agent. In this experiment, all the glass ware used was acid washed. The chemical reagents used were analytical reagent grade which needs no further purification. Ultrapure water was used for all dilution and sample preparation. All the fabrication process was done at room temperature.

B. Sample preparation

In a typical experiment, 2.2 g (0.2 mol/l) of zinc acetate Zn (CH₃COOH)₂.2H₂O was dissolved in 50 ml deionised water. The stirring rate of solution was taken as 1200 rpm at room temperature. Then 1 gm of PVP was dissolved in 50 ml deionised water and was added drop by drop to the constant stirring solution for stabilizing the synthesized particles. The mixture was stirred at room temperature until a homogeneous solution was obtained. After that 0.4 gm (0.2 mol/l) of 50 ml sodium hydroxide was added drop by drop to the above mixture which gives white voluminous precipitate. The stirring process was continued for 3 hours till a white precipitate deposited at the bottom of the beaker. This solution was kept overnight for settlement of precipitate. Then the precipitate was filtered and washed 2-3 times with distilled water and 1-2 times with absolute ethanol by using Whatmann filter paper. After this process finally the products were dried in hot air oven at 100 °C for 1 hour. The powder obtained was used for further characterization process.

C. Characterization

The X-Ray Diffraction (XRD) patterns of the undoped ZnO sample was recorded by XPERT-PRO Diffractometer system using CuK α radiation ($\lambda=1.54056$ Å) at 45 kV and 40 mA. The morphology and size of the particles were determined by Scanning Electron Microscopy (SEM) by using JEOL-EO microscopy with The interplaner spacing (d) is evaluated using the relation (1) as explained by [26] which is given in **table 1**.

$$\frac{1}{d^2} = \frac{4}{3} \left(\frac{h^2 + hk + k^2}{a^2} \right) + \frac{l^2}{c^2} \quad (1)$$

Where a and c is the lattice constant defined as follows:

$$a = \frac{\lambda}{\sqrt{3} \sin \theta} \quad (2)$$

For (100) plane, the lattice constant a is calculated by using equation (2) as explained by [27] and found to be a=3.2428 Å .

$$c = \frac{\lambda}{\sin \theta} \quad (3)$$

accelerating voltage 20 kV. The optical absorption spectra of the particles were recorded using Perkin Elmer Lambda -45 spectrophotometer in the wavelength range 200-800 nm.

III. RESULTS AND DISCUSSIONS

A. Structural studies

A typical XRD pattern of the prepared nanorods is shown in **fig.1**. The pattern obtained is indexed with hexagonal unit cell structure with wurtzite structure (JCPDS Card no. 36-1451). The observed relative peak intensities and interplaner spacing has been compared to that of their standard values which is given in **table 1**. All peaks of the obtained product correspond to the hexagonal wurtzite structure of Zn which is studied by many researchers. In **fig.1**, the detected peaks are at 2 θ values of 31.8384°, 34.4937°, 36.40840°, 47.57920° and 56.65420° corresponding to the following lattice planes (100), (002), (101), (102) and (110). It has been observed that there is a small difference in the relative peak intensities of the lattice planes (100) to (002) and in the d- spacing of different peaks. Also, it has been seen that the XRD patterns of the nanorods are considerably broad because the crystals are randomly arranged or have low degree of periodicity. Furthermore no impurities were found in XRD pattern. This result shows that high purity hexagonal ZnO nanorods could be obtained by this chemical method.

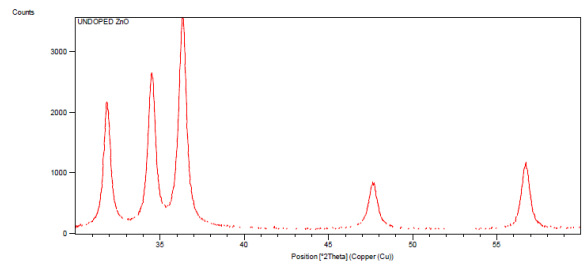


Fig.1: XRD pattern of undoped ZnO nanorods.

Similarly, for (002) plane, lattice constant c is calculated by using equation (3) as explained by [27] and found to be c=5.1960 Å .

Hence, the ratio c/a=1.6023. Also, the diffraction peaks corresponding to the planes (100), (002), (101), (102) and (110) are obtained from X-ray diffraction data which are consistent with the JCPDS data of ZnO. The interplaner spacing (d) calculated from XRD is compared with JCPDS data card and corresponding (h k l) planes are summarized in **table 1**.

The crystalline size (D) is calculated by Debye-Scherrer formula using raw data from XRD patterns. The formula is given in relation (4) and the calculated values are given in **table 2**.

$$D = \frac{k\lambda}{\beta \cos \theta} \quad (4)$$

Where k is constant (0.9), D is the crystalline size (in nm), λ is wavelength (0.15406 nm), β is Full Width at Half Maximum (FWHM in radian) intensity and θ is the Bragg diffraction angle [28].

Quantative information concerning the preferential crystal orientation can be obtained from the Texture coefficient (T_c), which is defined as in relation (5) given by [29].

$$T_c(hkl) = \frac{I(hkl)/I_o(hkl)}{\frac{1}{n} \sum_n [I(hkl)/I_o(hkl)]} \quad (5)$$

Where T_c (hkl) is the Texture coefficient, I (hkl) is the XRD intensity, n is the number of diffraction peaks considered and I_o (hkl) is the standard intensity of the plane which is taken from JCPDS data as given by [30, 31].

If $T_c(hkl) \approx 1$ for all the (hkl) planes considered then the particles are randomly oriented crystallites which is similar to the JCPDS references. If the values of $T_c(hkl)$

Table 1: Comparison of the X-Ray Diffraction peak intensities, 2θ , d-values, and d% error of the JCPDS data from the observed data.

XRD Peak (hkl)	2θ (degree) observed	2θ (degree) from JCPDS	Intensity observed	Intensity from JCPDS	d-spacing observed (Å)	d-spacing from JCPDS (Å)	Texture Coefficient $T_c(hkl)$	Relative percentage error
100	31.8384	31.770	61.64	57	2.80842	2.81430	1.11	0.21%
002	34.4937	34.422	76.20	44	2.60022	2.60332	1.7	0.11%
101	36.4084	36.253	100	100	2.46775	2.47592	1.03	0.33%
102	47.5792	47.539	21	23	1.91120	1.91114	0.94	0.003%
110	56.6542	56.603	30.60	32	1.62337	1.62472	0.98	0.083%

The ZnO bond length L is given by equation (7) as explained by [34] is shown in **table 2**.

$$L = \sqrt{\frac{a^2}{3} + \left(\frac{1}{2} - u\right)^2 c^2} \quad (7)$$

Where, u is the positional parameter in the wurtzite structure which relates to c/a ratio. u is a measure of the amount by which each atom is displaced with respect to the next along the 'c' axis and is given by,

$$u = \frac{a^2}{3c^2} + 0.25$$

The dislocation density (δ) as given by Williamson Smallman's formula represents the amount of defects in the powder which is determined by relation (8) shown in **table 3**. The larger D and smaller FWHM values indicate better crystallization of the particles [35].

is greater than 1, it indicates that the abundance of grain is formed in a given (hkl) direction. If $0 < T_c(hkl) < 1$ it indicates that there is lack of grains in that given directions. As $T_c(hkl)$ increases, the preferential growth of the crystallites in the direction perpendicular to the (hkl) plane is greater. This is given in **table 1**.

The relative percentage error for all the particles has been evaluated by equation (6) and JCPDS standard d-values as given by [32] which are shown in **table 1**.

$$\text{Relative percentage error} = \frac{Z_H - Z}{Z} \times 100\% \quad (6)$$

Where Z_H is the actual obtained d-value in XRD pattern, Z is the standard d-value in JCPDS data. The values of 2θ , d-values, and d% error for the crystalline ZnO nanorods are calculated by using equation (4) and given in **table 1**. The average relative percentage error is found to be 0.21%, 0.11%, 0.33%, 0.003% and 0.083% respectively. The experimental d-values and JCPDS d-values are approximately equal and show hexagonal structure [33].

$$\delta = \frac{1}{D^2} \quad (8)$$

The volume (V) of hexagonal cell given by equation (9) is calculated and shown in **table 2** [36].

$$V = \frac{\sqrt{3}}{2} a^2 c \quad (9)$$

The strain (ϵ) induced in powders due to crystal imperfection and distortion has been calculated by Williamson Hall method using equation (10) and line breadth ($\beta_{hkl} \cos \theta$) is calculated by equation (11) which is shown in **table 2** [37].

$$\epsilon = \frac{\beta_{hkl}}{4 \tan \theta} \quad (10)$$

$$\beta_{hkl} \cos \theta = \frac{k\lambda}{D} + 4\epsilon \sin \theta \quad (11)$$

Table 2: Volume, Bond length, Strain, Line breadth, FWHM and particle size

Volume(V) $(\text{Å})^3$	Bond length(L) (Å)	Strain ϵ	Line breadth $\beta_{hkl}\cos\theta$	FWHM(β) in degree	Particle Size D(nm)
51.151	2.0281	0.007273	0.009503	0.1020	91
40.496	1.8763	0.014281	0.020002	0.1840	45.23
34.618	1.7807	0.017882	0.025949	0.2175	38.47
16.080	1.3791	0.036876	0.064840	0.3346	25.96
9.879	1.2052	0.060482	0.121686	0.4488	20.12

Integral breadth (β) of ZnO has been obtained from XRD patterns using relation (12) which is given in **table 3** [38].

$$\beta = \frac{\text{Area}}{I_o} \quad (12)$$

Where, Area = area under peak

I_o = maximum intensity

The Lorentz-polarization factor is the most important of the experimental quantities that control X-ray intensity with respect to diffraction angle. In the intensity calculations Lorentz factor is combined with the **Table 3:** Dislocation density, Integral breadth, Lorentz factor and Lorentz polarization factor

Dislocation density (δ) $(\text{nm})^{-2}$	Integral breadth (β)	Lorentz factor	Lorentz polarization factor
0.000120758	2.3772	3.4557	23.7987
0.000535093	4.5163	2.9778	20.0026
0.000675702	7.0045	2.6965	17.7724
0.001483852	2.3407	1.6791	9.7726
0.002470267	5.9797	1.2614	6.5701

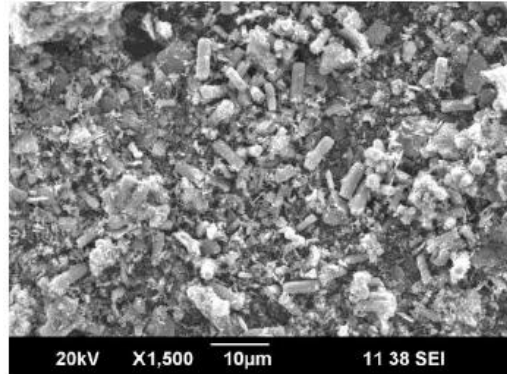
B. Morphological study

Fig.2 represents the SEM image of ZnO nanorods at different magnifications. These pictures confirm the formation of ZnO nanorods. It is clear from the **fig. 2(a)** that the size of nanorods is $10 \mu\text{m}$ at low magnification. From the amplified SEM image it is clear that the ZnO nanorod is hexagonal in structure as shown in **fig.2(b), (c) and (d)**. The powder contains ZnO nanorods of diameter $1.52 \mu\text{m}$ - $1.61 \mu\text{m}$ and of length $4.89 \mu\text{m}$. In this work, the two main reactants used to fabricate ZnO are NaOH and $\text{Zn}(\text{CH}_3\text{COO})_2 \cdot 2\text{H}_2\text{O}$. The solubility of these reactants in water (109 and 30) is much higher than other solvent. The high solubility is the main factor which decreases the number of nucleation sites [42]

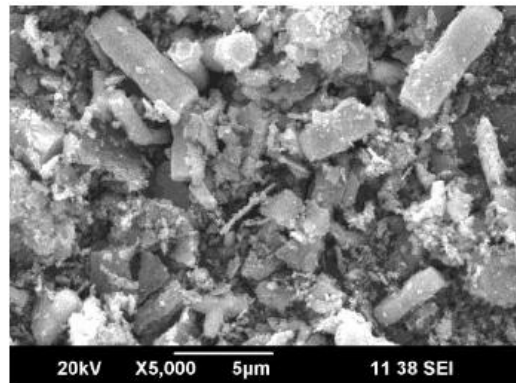
polarization factor and further the variation of the Lorentz's factor with the Bragg angle θ [39]-[41]. The overall effect of Lorentz factor is to decrease the intensity of the reflections at intermediate angles compared to those in the forward or backward directions. Lorentz factor and Lorentz polarization factor are calculated from equation (13) and (14), is shown in **table 3**.

$$\text{Lorentz factor} = \frac{\cos \theta}{\sin^2 2\theta} = \frac{1}{4 \sin^2 \theta \cos \theta} \quad (13)$$

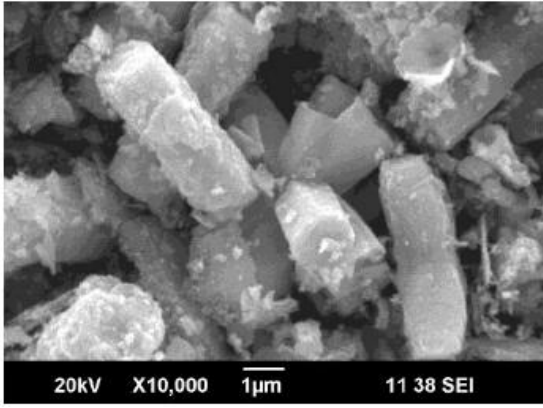
$$\text{Lorentz polarization factor} = \frac{1 + \cos^2(2\theta)}{\sin^2 \theta \cos \theta} \quad (14)$$



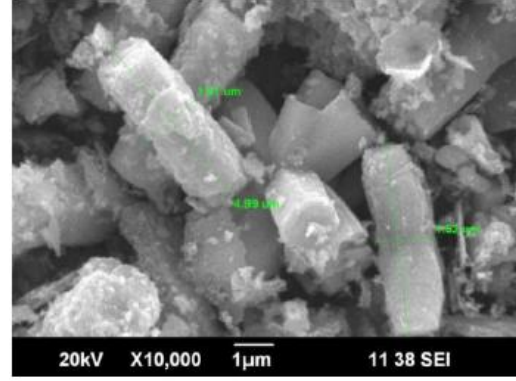
(a)



(b)



(c)



(d)

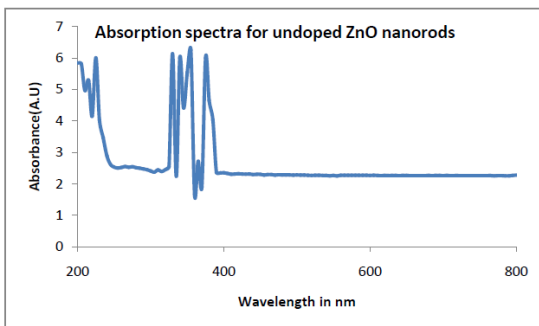
Fig.2: (a) low and (b), (c) and (d) high- magnification SEM images of undoped ZnO nanorods.

C. Optical properties

UV-VIS absorption spectra of the ZnO nanorods are shown in **fig.3**. The optical properties are strongly dependent on the particle size. The room temperature spectra exhibit strong excitonic absorption peak at 355 nm. The absorption spectrum shows a well defined exciton band at 355 nm and significant blue shift relative to the bulk exciton absorption (373 nm) [43]. This blue shift phenomenon is mainly related to the quantum confinement effect of the small size of ZnO [44]. The most direct way of extracting the optical bandgap is to simply determine the photon energy at which there is sudden increase in the absorption. For bulk samples, the bandgap is estimated from the $(\alpha h\nu)^2$ vs $(h\nu)$ plot, where α is the absorption coefficient and $h\nu$ is the photon energy. But for nanocrystalline samples the bandgap is determined from absorption maxima. The optical bandgap E_g of the nanocrystalline samples are calculated from the absorption peak using the formula,

$$E_g = hc/\lambda$$

where h is plank's constant, c is the velocity of light and λ is the wavelength of the light at which absorption peak is obtained. The bandgap of ZnO has been found to be 3.4 eV.


Fig.3: UV- Visible absorption spectrum of undoped ZnO nanorods.

The average particle size in a nanocolloid can be calculated from the absorption onset of UV-VIS

absorption spectra (**fig.3**) by using effective mass model [45]-[46] where the bandgap E^* can be approximated by:

$$E^* = E_g^{bulk} + \frac{\hbar^2 \pi^2}{2er^2} \left(\frac{1}{m_e^* m_0} + \frac{1}{m_h^* m_0} \right) - \frac{1.8e}{4\pi\epsilon_0 r} - \frac{0.124e^3}{\hbar^2 (4\pi\epsilon_0)^2} \left(\frac{1}{m_e^* m_0} + \frac{1}{m_h^* m_0} \right)^{-1} \quad (15)$$

where E_g^{bulk} is the bulk bandgap expressed in eV, \hbar is Plank's constant, r is a particle radius, m_e is the electron effective mass, m_h is the hole effective mass, m_0 is free electron mass, e is the charge on the electron, ϵ is the relative permittivity and ϵ_0 is the permittivity of free space. Due to the relatively small effective masses for ZnO ($m_e = 0.26$, $m_h = 0.59$) bandgap enlargement is expected for particle having radii less than about 4 nm [44, 45]. The following equation has been derived from the effective mass model given above with small mathematical simplification [47] which is used to find the size of the particle from the absorbance spectra.

The average particle size present in the nanoparticles can be determined by using the mathematical model of effective mass approximation equation (16) as explained by [48]-[49].

$$r(nm) = \frac{-0.3049 + \sqrt{-26.23012 + \frac{10240.72}{\lambda_p(nm)}}}{-6.3829 + \frac{2483.2}{\lambda_p(nm)}} \quad (16)$$

Where r is radius of the particle size, λ_p is the peak absorbance wavelength for monodispersed ZnO nanoparticles, $m_e = 0.26 m_0$, $m_h = 0.59 m_0$, m_0 is the free electron mass, $\epsilon = 8.5$ and $E_g^{bulk} = 3.3$ eV. The prepared ZnO nanorods show absorbance peak at 355 nm which corresponds to average particle size of 2.15 nm.

IV. CONCLUSIONS

ZnO nanorods with diameter 1.52 μm -1.61 μm and length of 4.89 μm respectively obtained by SEM has been successfully prepared by a simple chemical precipitation method at room temperature. In this sample preparation zinc acetate dihydrate was used as a precursor and poly vinyl pyrrolidone was used as a

capping agent. The XRD patterns obtained confirms the formation of wurtzite hexagonal ZnO nanostructures without any impurities. The XRD studies of these nanorods revealed that their average size is about 49 nm for undoped ZnO which is calculated by Debye Scherrer formula. Also, d-spacing and relative peak intensities have been compared from their standard values. Relative intensity at lattice plane (101) and d-spacing for lattice planes (102) and (110) were found nearly equal. It can be seen that the highest texture coefficient is in (101) plane for undoped ZnO. The bond length of 1.7151 Å has been related with ZnO unit cell. The size and strain contribution to line broadening has been analyzed by the method of Williamson and Hall. Further, the UV absorption at ~ 355 nm is found which is blue shifted; energy bandgap of ZnO is calculated as 3.4 eV. From UV-Visible absorption spectra, the calculated average size of prepared undoped ZnO nanorods is found to be 2.44 nm for peak absorption wavelength. Hence, it is concluded that in the presence of deionised water as solvent, the size of ZnO nanorods is in micro range.

ACKNOWLEDGEMENT

Authors are thankful to SAIF Kochi, Ernakulam for characterization of samples by SEM technique, SAIF Panjab University, Chandigarh for XRD studies and CIL Panjab University for UV-Visible absorption spectra of the given samples.

REFERENCES

- [1] A.M Morales and C.M.Lieber, *Science*, 279, 208 (1998) DOI:10.1126/science.279.5348.208
- [2] H.Dai, E.W. Wong, Y.Z. Lu, F. Shoushan and C.M. Lieber, *Nature*, 375, 769 (1995). DOI: 10.1038/375769a0
- [3] W.Q Han, S.S Fan, Q.Q. Li and Y.D.Hu, *Science*, 277, 1287 (1997). DOI:10.1126/science.277.5330.1287
- [4] J.H Zhan, X.G Yang, D.W Wang, S.D Li, Y Xie, Y.N Xia and Y.T Qian, *Adv. Mater.*, 12, 1348 (2000). DOI:10.1002/1521-4095(200009)
- [5] Hu, J.T., Odom, T.W. and Lieber, C.M. *Acc. Chem. Res.*, 32, 435 (1999). DOI:10.1021/ar9700365
- [6] R. Radheshyam, *Adv. Mat. Lett.*, 1(1), 55 (2010). DOI:10.5185/amlett.2010.3101
- [7] L.Chen, X Pang, Y. Guangshui and J.Zhang, *Adv. Mat. Lett.*, 1(1), 75 (2010). DOI:10.5185/amlett.2010.4117
- [8] S. Gautam, S. Kumar, P. Thakur, K.H Chae, R. Kumar, B.H. Koo and C.G Lee, *J. Phys. D: Appl. Phys.*, 42, 175406 (2009). DOI:10.1088/0022-3727/42/17/175406
- [9] A. Azam, F. Ahmed, N. Arshi, M.Chaman and A.H. Naqvi, *J. Alloys and Compounds*, 496, 399 (2010). DOI:10.1016/j.jallcom.2010.02.028
- [10] S. Kumar, G.W. Kim, B.H. Koo, S.K. Sharma, M. Knobel, H. Chung and C.G. Lee, *J. Nanosci. Nanotechnol.*, 11, 555 (2011). DOI:10.1166/jnn.2011.3176
- [11] S.Kumar, Y.J. Kim, B.H. Koo, C.G. Lee, *J. Nanosci. Nanotechnol.*, 10, 7204 (2010). DOI:10.1166/jnn.2010.2751
- [12] S.Kumar, Y.J. Kim, B.H. Koo, H.K. Choi and C.G. Lee, *IEEE Transaction on Magnetics*, 45, 2439 (2009). DOI:10.1109/TMAG.2009.2018602
- [13] S.Kumar, Y.J. Kim, B.H. Koo, S.K. Sharma, M.Knobel, C.T. Meneses, D.K.Shukla, R.Kumar and C.G. Lee, *J. Korean Phys. Soc.*, 55, 10108-1021 (2009). DOI:10.3938/jkps.55.1018
- [14] Y.K. Park, J.InHan, M.G. Kwak, H.Yang, S.H. Ju, and W.S. Cho, *J. Lumin.*, 78, 87 (1998). DOI: 10.1016/S0022-2313(97)00277-9.
- [15] Q.X. Zhao, M. Willander, R.E. Morjan, Q-H.Hu and E.E.B. Campbell *Appl.Phys.Lett.*, 83, 165-167 (2003).
- [16] K. Elmer *J.Phys. D: Appl.Phys.*, 33, R 17 (2000).
- [17] M. Krunk and E. Mellikov, *Thin Solid Films*, 270, 33 (1995).
- [18] J.A. Aranovich, D.Golmayo, A.L.Fahrenbruch and R.H.Bube. *J.Appl.Phys.*, 51, 4260 (1980).
- [19] U.Ozgur, Y. I.Alivov, C.Liu, A.Teke, M.A.Reshchikov, S.Dogan, V.Avrutin, S.-J. Cho and H.Morkoc. *J.Appl.Phys.*, 98, 04130 (2005)
- [20] Jih-Jen Wu and Sai-Chang Liu, *Adv. Mater.*, 14, 215 (2002).
- [21] A. Fouchet, W. Prellier and B. Mercey, L.Mechin, V.N.Kulkarni and T.Venktesan. *J. Appl. Phys.*, 96, 3228 (2004).
- [22] H. Takikawa, K. Kimura, R. Miyano and T. Sakakibara. *Thin Solid Films.*, 377-378, 74-80, (2000).
- [23] Q. P. Wang, D. H. Zhang, Z. Y. Xue and X. T. Hao, *Applied Surface Science*, 201, 123 (2002).
- [24] Hanmei Hu et al, *Materials Chemistry and Physics*, 2007, 106, 58.
- [25] A. Eftekhari, F. Molaei and H. Arami, *Materials Science and Engineering A*, 437, 446, (2006).
- [26] M. Mazhdi and P. HosseinKhani, "Structural characterization of ZnO and ZnO:Mn nanoparticles prepared by reverse micelle method", *Int.J.NanoDim.*, 2(4): 233-240 (2012).

- [27] Cullity, B.D., Stock, S.R.: Elements of X-ray diffraction, 3rd edn. Prentice Hall, New Jersey (2001)
- [28] A.Khorsand Zak, W.H Abd. Majid., M.E. Abrishami and R. Yousefi, X-ray analysis of ZnO nanoparticles by Williamson-Hall and size-strain plot methods. *Solid State Sciences*. 13:251-256(2011).
- [29] S.Ilican, Y.Caglar, M.Caglar, "Preparation and characterization of ZnO thin films deposited by sol-gel spin coating method". *Journal of optoelectronics and advanced materials*., 10:2578–2583(2008).
- [30] Joint Committee on Powder Diffraction Standards, Powder Diffraction File, Card No: 891397.
- [31] H. Schulz and K. H. Thiemann, "Structure Parameters and Polarity of the Wurtzite Type Compounds SiC-2H and ZnO ," *Solid State Communications*, Vol. 32, No. 9, pp. 783-785(1979).
- [32] D. PathinettamPadiyan and A. Marikani, "X-Ray Determination of Lattice Constants of CdXSn1-XSe Mixed Crystal Sys-tems," *Crystal Research and Technology*, Vol. 37, No. 11, pp. 1241-1248(2002). DOI:10.1002/1521-4079(200211)37:11<1241::AID-CRAT1241>3.0.CO;2-C.
- [33] Joint Committee on Powder Diffraction Standards, Powder Diffraction File, card no: 36-1451.
- [34] F. Yakuphanoglu, S. Ilican, M. Caglar, Y. Caglar, The determination of the optical band and optical constants of non-crystalline and crystalline ZnO thin films deposited by spray pyrolysis, *J.Optoelectron. Adv. Mater.*, Vol. 9, pp.2180-2185(2007).
- [35] G.B. Williamson, R.C. Smallman, *Philos. Mag.*, Vol 1, , pp. 34(1956).
- [36] C. Kittel, "Introduction to Solid State Physics," 8th Edition, John Wiley & Sons, New York, (2005).
- [37] R. Yogamalar, R. Srinivasan, A. Vinu, K. Ariga and A.C. Bose, *Solid State Commun.*,149, 1919(2009).
- [38] P. Sutta and Q. Jackuliak, *Mater. Struct.*,5, 10(1998).
- [39] H. S. Peiser, H. P. Rooksby and A. J. C. Wilson, "X-Ray Diffraction by Polycrystalline Materials," The Institute of Physics, London, (1955).
- [40] G. L. Clark, "Applied X-Rays," 4th Edition, McGraw- Hill Book Company, Inc., New York, (1955).
- [41] A. H. Compton and S. K. Allison, "X-Rays in Theory and Experiment," D. Van Nostrand Company, Inc., New York, 1935.
- [42] J. Zhao, X. Yan, Y. Lei, Y. Zhao, Y. Huang and Y. Zhang, *Adv.Mate.Res.*1,1 75-81(2012).
- [43] M.Haase, H.Weller, A.Henglein, *J.Phys.Chem.*,92, 482(1988).
- [44] U.Koch, A.Fojtik, H.Weller, A.Henglein, *Chem.Phys.Lett.* , 122 507(1985).
- [45] S. Shionoya and W. M. Yen, Eds., *Phosphor Handbook*, CRC Press, Boca Raton, Fla, USA, (1998).
- [46] L. I. Berger, *Semiconductor Materials*, CRC Press, Boca Raton, Fla, USA, (1997).
- [47] L. Brus, "Electronic wave functions in semiconductor clusters: experiment and theory," *Journal of Physical Chemistry*, vol. 90, no. 12, pp. 2555–2560, (1986).
- [48] N. S. Pesika, K. J. Stebe and P. C. Searson, "Determination of the Particle Size Distribution of Quantum Nano- crystals from Absorbance Spectra," *Advanced Materials*, ,Vol. 15, No. 15, pp. 1289-1291(2003). DOI:10.1002/adma.200304904
- [49] L. Brus, "Electronic Wave Functions in Semiconductor Clusters: Experiment and Theory," *The Journal of Physical Chemistry*, Vol. 90, No. 12, pp. 2555-2560(1986). DOI: 10.1021/j100403a003

